Tellus (2006), 58A, 196–209

TELLUS

The representation of the analysis effect in three error simulation techniques

By LOÏK BERRE[1], SIMONA ECATERINA ŞTEFĂNESCU[2*] and MARGARIDA BELO PEREIRA[3], [1]*Météo France, CNRM/GAME-GMAP, Toulouse, France;* [2]*National Meteorological Administration, SMDCA, Bucharest, Romania;* [3]*Instituto de Meteorologia, Departamento de Vigilância Meteorológica, Lisbon, Portugal*

(Manuscript received 17 February 2005; in final form 30 September 2005)

ABSTRACT

Three error simulation techniques are compared formally, in particular regarding their representation of the analysis step. The associated results are moreover examined for the Aladin-France limited-area model, which is coupled with the Arpège global model.

It is first shown that the analysis error equation involves the same operators as the analysis equation. This implies that the analysis ensemble approach is appropriate, as the analysis equation is used to transform the background and observation dispersions into the analysis dispersion.

By contrast, the standard NMC method relies essentially on the analysis increment equation, which contributes to a large extent to the excessive emphasis on the large-scale structures. The so-called lagged NMC method is shown to be closely related to the Arpège/Aladin model differences.

The analysis ensemble approach gives error spectra that are intermediate between those of the two other methods. This is in agreement with the representation of the initial and lateral boundary uncertainties, in a way that is consistent with the influence of the analysis equation and with the short forecast ranges.

1. Introduction

Data assimilation schemes, such as three-dimensional variational systems (3D-Var), combine observations and a background, which is for instance a 6-h forecast. In such schemes, the background error covariances determine the filtering and the propagation of the observed information. Nevertheless, the estimation of these error covariances is not straightforward, for example, because the truth is never exactly known.

In this study, a method based on an ensemble of analyses is compared to two other simulation techniques, which are two variants of the NMC (National Meteorological Center, nowdays named National Center for Environmental Prediction) method (the so-called "standard" and "lagged" versions of the NMC method, according to the terminology of Široká et al., 2003). These three methods will be compared formally, with respect to the equations of the error evolution. In particular, the representation of the analysis step will be examined. This will allow to highlight the strong role of the analysis equation in the exact error evolution and in the ensemble simulation. The contrast between this and the involvement of the analysis increment equation in the NMC method will be made explicit and discussed. Moreover, some experimental results will be presented for the Aladin limited-area model (LAM) (Bubnová et al., 1993; Radnóti et al., 1995) which is coupled with the Météo France global model Arpège.

Techniques such as the NMC method are used in many NWP (Numerical Weather Prediction) centres, but the related formalism and approximations are not often explicit. The long forecast ranges of the NMC method (e.g. 12 and 36 h) are a well-known drawback. In the present paper, the analysis step representation will be shown to be another critical component in the error simulation.

Some efforts to derive the implicit formalisms have nevertheless been done in the past. For instance, the formalism of the (standard) NMC method is made explicit and discussed in Bouttier (1994). The equations are presented in matrix form, and they concern essentially the covariance matrix equation of the first analysis increment. We propose therefore to explicit the NMC formalism in vector form (which facilitates, e.g., the comparison with the ensemble formalism), and also to extend the discussion to the addition of several analysis increments (which is usually involved).

[*] Corresponding author.
e-mail: simona.stefanescu@meteo.inmh.ro
DOI: 10.1111/j.1600-0870.2006.00165.x

The results of the method based on an ensemble of analyses are described in Houtekamer et al. (1996) and Fisher (2003). A description of the corresponding formalism is presented in Žagar et al. (2004). The formalism of this approach will be established here in a partly different way, in the sense that it will be based on the usual BLUE ("best linear unbiased estimator") equation. Firstly, this facilitates the comparison with the NMC method. Secondly, this will show that the analysis equation can be applied to the error fields, even if the prescribed statistics and actual observation operator are not exact.

The formalism of the lagged NMC method will also be made explicit and discussed. It will be shown that this approach relies strongly on the Arpège/Aladin model differences (without a proper representation of the initial and lateral boundary uncertainties).

The paper is organized as follows: In Section 2, the equations that govern the evolution of the model state errors are derived, in particular to highlight the role of the analysis equation. Section 3 describes the corresponding equations for the evolution of the model state differences in the ensemble error simulation method. A similar involvement of the analysis equation is in particular pointed out. Section 4 deals with the implicit formalism of the standard NMC method. This allows to exhibit the strong role of the analysis increment equation. The associated formal expectations are then examined experimentally in Section 5, by comparing the Aladin-France results of the ensemble and standard NMC methods. In Section 6, the link between the lagged NMC method and the Arpège/Aladin model differences is examined, and the variance spectra of the three simulation methods are compared. Conclusions and perspectives are outlined in Section 7.

2. The evolution of the model state errors

The equations that govern the evolution of the model state errors (i.e. the analysis errors and the background errors) will be derived. This will allow later on (Sections 3 and 4) to explain the different representations of the analysis step in the ensemble and standard NMC methods. It will be shown that this analysis step difference contributes much to the experimental differences between the ensemble and standard NMC techniques in the Arpège/Aladin system (Section 5).

For simplicity, in the forecast and analysis steps, the operators will be considered to be linear. Similar equations can be derived in a non-linear framework, for example, by introducing some Taylor developments (Žagar et al., 2004).

2.1. The forecast step

At time t_i, the analysis x_a^i is an estimate of the true atmospheric state x_*^i, with uncertainties that correspond to the analysis error $e_a^i = x_a^i - x_*^i$.

The 6-h forecast field x_b^{i+1}, that is valid at time $t_{i+1} = t_i + 6h$, is then obtained from this initial condition x_a^i, by integrating in time the forecast model, according to: $x_b^{i+1} = Mx_a^i$, where M is the operator that corresponds to the 6-h evolution which is provided by the forecast model. The true fields will evolve according to: $x_*^{i+1} = M_* x_*^i$, where M_* is the exact 6-h forecast operator. This gives the following expression for the background errors $e_b^{i+1} = x_b^{i+1} - x_*^{i+1}$:

$$e_b^{i+1} = M e_a^i + e_m^{i+1}, \tag{1}$$

where e_m^{i+1} is the 6-h accumulated model error (see, e.g., Daley, 1991, p. 376): $e_m^{i+1} = (M - M_*)x_*^i$.

2.2. The analysis step

The 6-h forecast field x_b^{i+1} will then be used as a background for the analysis at time t_{i+1}. The analysis equation is the equation that transforms the background and observation vectors into the analysis vector:

$$x_a^{i+1} = x_b^{i+1} + \mathbf{K}\big(y^{i+1} - H x_b^{i+1}\big), \tag{2}$$

where y^{i+1} is the observation vector at time t_{i+1}, H is the observation operator, and $\mathbf{K}$ is the classical gain matrix, namely, $\mathbf{K} = \mathbf{B}\, H^T(H\mathbf{B}H^T + \mathbf{R})^{-1}$. $\mathbf{B}$ and $\mathbf{R}$ are the specified spatial covariance matrices of the background errors and of the observation errors, respectively, and the exponent^T is a notation for the adjoint operator.

It is then possible to consider the application of the analysis equation to x_*^{i+1} as a background field, and to $y_{*,H}^{i+1} = Hx_*^{i+1}$ as an observation vector. The vector $y_{*,H}^{i+1}$ is the projection of this true field onto the observation space, that is provided by the observation operator H. As the definition of $y_{*,H}^{i+1}$ implies that $y_{*,H}^{i+1} - Hx_*^{i+1} = 0$, it appears that the analysis equation applies well to the previous two fields:

$$x_*^{i+1} = x_*^{i+1} + \mathbf{K}\big(y_{*,H}^{i+1} - H x_*^{i+1}\big). \tag{3}$$

The result $\mathbf{K}(0) = 0$ is valid as $\mathbf{K}$ is linear. More generally, this is also the case for a non-linear analysis, if the analysis does not modify the background field, when the observations are exactly consistent with the background (i.e. when the observation vector is equal to Hx_b^{i+1}).

By calculating the difference between the last two equations, it becomes obvious that the analysis equation is also the equation that transforms the background and observation errors into the analysis errors (note that the related operators are the same as in eq. 2):

$$e_a^{i+1} = e_b^{i+1} + \mathbf{K}\big(e_o^{i+1} - H e_b^{i+1}\big), \tag{4}$$

where $e_o^{i+1} = y^{i+1} - y_{*,H}^{i+1} = y^{i+1} - Hx_*^{i+1}$ is the observation error (which is itself the sum of the measurement error $e_{om}^{i+1} = y^{i+1} - y_*^{i+1}$, and of the representativeness error $e_{or}^{i+1} = y_*^{i+1} - y_{*,H}^{i+1} = y_*^{i+1} - Hx_*^{i+1}$, where y_*^{i+1} is the exact atmospheric state in the observation space).

It may be interesting to notice also that the derivation of the analysis error expression does not require the assumption that the analysis is perfect: in particular, the gain matrix **K** may be suboptimal (i.e. the specified error covariance matrices **B** and **R** can be different from the exact ones), and the observation operator may be erroneous.

3. The ensemble simulation method

The ensemble method that has been used, for example, by Houtekamer et al. (1996) and by Fisher (2003) consists in simulating the evolution of the model state errors. This is realized by introducing and evolving some perturbations, which have similar statistical features as the error contributions.

This approach may be described formally when considering the difference between two members of the ensemble, which will be referred to by the indices k and l.

3.1. The forecast step

At time t_i, two different analyses $x^i_{a,k}$, $x^i_{a,l}$ are available. Their difference is equal to $\varepsilon^i_a = x^i_{a,k} - x^i_{a,l}$.

Two forecast integrations are performed from these two initial states. Moreover, some model perturbations $\delta^{i+1}_{m,k}$, $\delta^{i+1}_{m,l}$ may be added, for instance at the end of the 6-h forecasts. This provides two 6-h forecast fields: $x^{i+1}_{b,k} = Mx^i_{a,k} + \delta^{i+1}_{m,k}$ and $x^{i+1}_{b,l} = Mx^i_{a,l} + \delta^{i+1}_{m,l}$. The difference between these two backgrounds, $\varepsilon^{i+1}_b = x^{i+1}_{b,k} - x^{i+1}_{b,l}$, reads

$$\varepsilon^{i+1}_b = M\varepsilon^i_a + \varepsilon^{i+1}_m \tag{5}$$

with

$$\varepsilon^{i+1}_m = \delta^{i+1}_{m,k} - \delta^{i+1}_{m,l}.$$

3.2. The analysis step

The two different 6-h forecast fields may then be combined with two different sets of observations y^{i+1}_k, y^{i+1}_l, in order to provide two different analyses at time t_{i+1}:

$$x^{i+1}_{a,k} = x^{i+1}_{b,k} + \mathbf{K}\left(y^{i+1}_k - Hx^{i+1}_{b,k}\right),$$

$$x^{i+1}_{a,l} = x^{i+1}_{b,l} + \mathbf{K}\left(y^{i+1}_l - Hx^{i+1}_{b,l}\right).$$

By calculating the difference between the last two equations, it appears that the analysis equation is the very same equation that transforms the background and observation differences into the analysis differences:

$$\varepsilon^{i+1}_a = \varepsilon^{i+1}_b + \mathbf{K}\left(\varepsilon^{i+1}_o - H\varepsilon^{i+1}_b\right) \tag{6}$$

where $\varepsilon^{i+1}_o = y^{i+1}_k - y^{i+1}_l$ is the vector of the observation differences. In practice, the two different sets of observations are obtained by adding two different perturbation vectors $\delta^{i+1}_{o,k}$, $\delta^{i+1}_{o,l}$ to the real observation vector y^{i+1}: $y^{i+1}_k = y^{i+1} + \delta^{i+1}_{o,k}$ and $y^{i+1}_l = y^{i+1} + \delta^{i+1}_{o,l}$.

The comparison between the equation pairs (1), (4) and (5), (6) is interesting: it indicates that the evolution processes and equations, that affect the ensemble difference fields, are the same as those of the true error fields.

In addition to this representation of the 6-h forecast and analysis effects, some other requirements are involved, in order to achieve a realistic error covariance estimation. This involves the perturbation covariances of the observations and of the model. This issue and its implications on the error covariance estimations are evoked in the appendix.

4. The standard NMC method

The NMC method (Parrish and Derber, 1992) computes differences between forecasts that are valid at the same time, but for different ranges, such as 12 and 36 h. The 36-h forecast may itself be seen as another 12-h forecast, whose initial condition is a 24-h forecast, instead of the operational analysis. This means that the initial differences between these two 12-h forecasts correspond to the effect of the four successive steps of analysis and 6-h forecast, which occur during the 24-h period.

We propose to write formally the related equations, in order to compare them with the evolution equations of the errors and of the ensemble differences.

4.1. The first assimilation cycle

At time t_i occurring 30 h before the verification time, there will be a first analysis step: the corresponding analysis increment $dx^i = x^i_a - x^i_b$ is the first difference that is introduced between the two integrations that will be compared.

This first analysis increment may be seen as an analysis perturbation ε^i_a, which is supposed to be an estimate of the analysis error e^i_a:

$$\begin{aligned}\varepsilon^i_a &= dx^i \\ &= \mathbf{K}\left(y^i - Hx^i_b\right) \\ &= \mathbf{K}\left(e^i_o - He^i_b\right)\end{aligned}$$

which allows to distinguish the respective contributions of the background and observation errors:

$$\varepsilon^i_a = -\mathbf{K}H\ e^i_b + \mathbf{K}\ e^i_o.$$

This can be compared to the exact analysis error equation (according to eq. 4):

$$e^i_a = (I - \mathbf{K}H)\ e^i_b + \mathbf{K}\ e^i_o,$$

and also to the analysis dispersion equation (following eq. 6):

$$\varepsilon^i_a = (I - \mathbf{K}H)\ \varepsilon^i_b + \mathbf{K}\ \varepsilon^i_o.$$

The matrices $I - \mathbf{K}H$ and $\mathbf{K}$ define the respective weights of the background and observation errors, in the analysis error equation. In the NMC method, the background error weight $I - \mathbf{K}H$ is approximated by $-\mathbf{K}H$.

As discussed by Bouttier (1994), this may be a reasonable approximation if $\mathbf{K}H \sim I/2$. This corresponds to the case where the observations are very dense (i.e. $H \sim I$), and the two error covariances are approximately the same ($\mathbf{R} \sim H\mathbf{B}H^T \sim \mathbf{B}$). The latter condition means that the observations are considered to have a similar quality and similar spatial error structures (i.e. similar error variances and correlations) as the background.

Nevertheless, in regions where data density is poor or where observations have a poor quality, the amplitude of the analysis increments is likely to be small, while the amplitude of the analysis error is large.

Moreover, the observation errors are usually much less correlated spatially than the background errors: the observation error spectrum tends to be white, while the background error spectrum is typically red. As discussed, for example, by Daley (1991, Section 4.5), this implies that the operator $\mathbf{K}H$ tends to act as a low-pass filter. Conversely, the operator $I - \mathbf{K}H$ is expected to act as a high-pass filter.

This implies that the analysis increment is likely to be of a larger scale than the analysis error. In other words, the analysis error correlations are expected to be overestimated by the NMC method.

The NMC analysis perturbation ε_a^i will evolve according to the forecast model during 6-h, which will provide a NMC background perturbation ε_b^{i+1}:

$$\begin{aligned}\varepsilon_b^{i+1} &= M\varepsilon_a^i \\ &= M\mathrm{d}x^i.\end{aligned}$$

4.2. The next three assimilation cycles

A second analysis step, which introduces some additional differences, will occur 24 h before the verification time. This amounts to considering that a new analysis increment will be added to the background perturbation (namely, $\varepsilon_b^{i+1} = M\varepsilon_a^i = Mdx^i$), in order to produce the following analysis perturbation:

$$\begin{aligned}\varepsilon_a^{i+1} &= M\,\mathrm{d}x^i + \mathrm{d}x^{i+1} \\ &= \varepsilon_b^{i+1} + \mathbf{K}\big(e_o^{i+1} - He_b^{i+1}\big).\end{aligned}$$

This last equation indicates that, in the evolution of the NMC perturbations, the representation of the analysis effect consists in *adding the analysis increment to some earlier increments* (for instance $\varepsilon_b^{i+1} = Mdx^i$ in the current case). This differs from the ensemble method, for which the representation of the analysis effect consists in *applying the analysis equation to the perturbations* ε_b, ε_o.

After the fourth analysis, the final NMC analysis perturbation is as follows:

$$\begin{aligned}\varepsilon_a^{i+3} &= \varepsilon_b^{i+3} + \mathrm{d}x^{i+3} \\ &= M^3\,\mathrm{d}x^i + M^2\,\mathrm{d}x^{i+1} + M\,\mathrm{d}x^{i+2} + \mathrm{d}x^{i+3},\end{aligned}$$

where M^j is the operator that corresponds to the forecast evolution during a period of $j \times 6$ h. ε_a^{i+3} corresponds to the 00 h-24 h differences.

The final 12-h evolution of the fourth analysis perturbation reads

$$\varepsilon_b^{i+5} = M^2\varepsilon_a^{i+3}.$$

4.3. The three specific components of the NMC method

In order to interpret the observed differences between the ensemble and NMC methods, one may therefore compare the following two synthetic equations. They summarize how the forecast differences (e.g. at time $i + 5$) are obtained, respectively, in the ensemble and NMC methods:

$$\varepsilon_b^{i+5} = M\ \varepsilon_a^{i+4},$$

$$\varepsilon_b^{i+5} = M^2\left(\sum_{j=1}^{4} M^{4-j}\ \mathrm{d}x^{i+j-1}\right).$$

These two equations allow to identify the main three specific components of the NMC method, compared to the ensemble method:

(i) the involvement of longer forecast ranges (see the occurrence of the matrices M^2, M^{4-j} instead of the 6-h matrix M);

(ii) the accumulation of several increments (see the occurrence of the operator $\sum$);

(iii) the involvement of analysis increments $\mathrm{d}x$, instead of analysis differences ε_a.

The respective contributions of these three components will be diagnosed experimentally in the next section.

5. Analysis ensemble against the standard NMC method: experiments

In this section, the results will be focused on the differences regarding the correlations and the contributions of different scales. This will illustrate the importance of the analysis step differences. The total variances will be presented later on in Section 6.3.

5.1. The Arpège/Aladin experiments

The results of the standard NMC method are compared to the results of the ensemble method over a 48-day period (February 4, 2002 to March 23, 2002), using fields valid at 12 UTC. The Aladin ensemble data set have been obtained in two steps. Firstly, an ensemble of Arpège global assimilation cycles has been performed in a perfect model framework (in accordance with the formal description in Section 3, and with $\varepsilon_m = 0$). The second step is the production of the ensemble of Aladin 6-h forecasts, with initial conditions and boundary conditions provided by the Arpège ensemble.

The Arpège assimilation system is a four-dimensional variational data assimilation (4D-Var) scheme (Veersé and Thépaut, 1998). The Arpège experiments have been done with its stretched version (i.e. the resolution is not uniform over the globe). The stretching factor is equal to 3.5, the truncation is T298 and there are 41 vertical levels. The Aladin model was integrated over the Aladin-France integration domain. The main geometrical characteristics for the Aladin-France integration domain are as follows: there are 41 vertical levels, the domain is square with lengths equal to $L_x = L_y = 2850$ km and the number of grid points in each direction is $J = K = 300$; the grid resolution is thus $\delta x = \delta y = 9.5$ km and the spectral truncation corresponds to $M = N = 149$ (M, N being the maximum wave numbers in each direction).

5.2. *Comparison between the two final statistics*

The respective error correlation spectra and correlation length scales, provided by the ensemble and (standard) NMC methods, are shown in Fig. 1. The correlation spectra are the variance spectra normalized by the total variance: they allow to compare the respective contributions of the different scales to the shape of the correlation functions.

The ensemble approach appears to provide error spectra that are shifted towards the small scales. As expected, this leads to smaller correlation length scales. The situation is nevertheless the opposite for the first 10–15 highest levels (near the tropopause and in the stratosphere). In particular, for temperature in the stratosphere, the ensemble method does not show the (unexplained) length scale decrease of the NMC method.

Moreover, the length scale differences are more pronounced for a large-scale variable such as temperature, than for a small-scale variable such as divergence. This is related to the larger differences in the large-scale part of the correlation spectra.

The larger emphasis on the small-scale contributions (by the ensemble method) is consistent with the results of Fisher (2003) over the globe, in which the NMC overestimation of the large-scale contributions was attributed to the long forecast ranges.

On the other hand, another explanation of the observed discrepancies between the ensemble and NMC methods could be the difference in the representation of the analysis effect.

5.3. *Diagnosis of the three elementary contributions in the NMC method*

Section 4 has shown that the NMC method involves three main components: the analysis increments, their accumulation, and their time evolution.

In order to diagnose the respective influences of these three ingredients, some correlation spectra have thus been examined at different stages of the two simulation techniques for surface pressure (Fig. 3). The uninitialized Arpège fields (projected onto the Aladin grid) have been used for comparison, in order to concentrate on the specific effects of the different steps of the NMC method. Moreover, it may be noticed that the typical NMC/ensemble contrast for the Aladin spectra (top left panel of Fig. 1) matches well with the contrast for the corresponding Arpège spectra (Fig. 2).

The top left panel of Fig. 3 allows to compare the spectrum of the “final” 36 h–12 h differences with the spectrum of the “initial” 00 h–24 h differences. The difference between these two spectra corresponds to the 12-h evolution of the initial differences. This 12-h evolution implies a slight increase of the relative contribution of the largest scales (at the expense of the contribution of the smaller scales).

The “initial” 00 h–24 h differences (which were described as the NMC analysis perturbations ε_a^{i+3} in Section 4.2) are themselves the result of the accumulation of four successive analysis increments, of which the first three evolve in time:

$$\begin{aligned}\varepsilon_a^{i+3} &= \sum_{j=1}^{4} M^{4-j}\, \mathrm{d}x^{i+j-1} \\ &= M^3\, \mathrm{d}x^i + M^2\, \mathrm{d}x^{i+1} + M\, \mathrm{d}x^{i+2} + \mathrm{d}x^{i+3}.\end{aligned}$$

It is therefore interesting to diagnose the effect of the successive forecast evolutions of the first three analysis increments. This has been done by plotting the spectrum of the sum of the four analysis increments:

$$\sum_{j=1}^{4} \mathrm{d}x^{i+j-1} = \mathrm{d}x^i + \mathrm{d}x^{i+1} + \mathrm{d}x^{i+2} + \mathrm{d}x^{i+3},$$

which amounts to replacing the forecast evolution matrices M^{4-j} by the identity matrix.

The spectrum of the 00 h–24 h differences and the spectrum of the sum of the four analysis increments are presented in the top right panel of Fig. 3. It appears that the evolutions of the (first three) increments contribute mostly to a slight enhancement of some intermediate large scales, corresponding to wave numbers between 4 and 20.

It is also possible to compare the spectrum of the increment sum $\sum_{j=1}^{4} \mathrm{d}x^{i+j-1}$ with the specific spectrum of each increment $\mathrm{d}x^{i+j-1}$. It appears (not shown) that the four increment spectra are very similar to each other, and that they are also close to the spectrum of the increment sum. Nevertheless, it may be mentioned that there is a slight enhancement of the contribution of the largest scales when the four increments are accumulated.

The bottom left panel of Fig. 3 allows to visualize the total effect of the forecast evolutions and of the analysis increment accumulation. This panel represents indeed the respective spectra of the 12 h–36 h forecast differences, and of the first analysis increment $\mathrm{d}x^i$. As expected, the forecast evolutions and the increment accumulation imply an increase of the large-scale contributions globally, compared to the small-scale contributions.

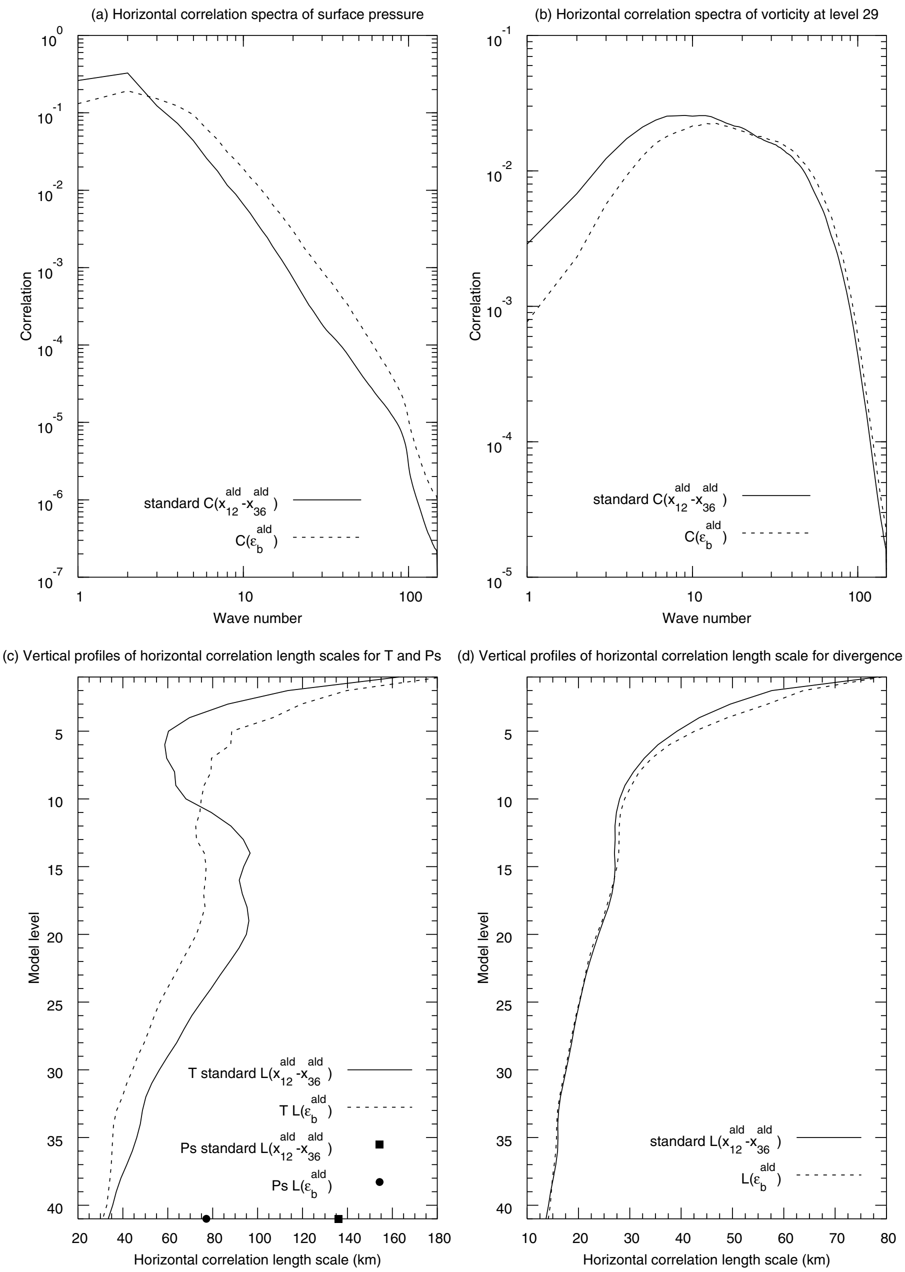

Fig. 1. The error correlation spectra (top panels) and the correlation length scales (bottom panels), for the Aladin standard NMC differences (full lines), and for the Aladin background ensemble differences (dotted lines). The model level 29 is located around the 775 hPa pressure level.

On the other hand, the relative contributions of some small wave numbers (such as 3 and 4) are slightly reduced, and the global differences between the two spectra are less strong than in Fig. 2.

It then appears interesting to compare (bottom right panel of Fig. 3) the analysis ensemble spectrum with the first analysis increment spectrum $\mathrm{d}x^i$ (of the NMC method). The discrepancy between these two curves corresponds to the influence of the differences (between the two simulation techniques) in the analysis effect representation.

The increment spectrum appears to be of a much larger scale than the analysis ensemble spectrum. This is consistent with the formal expectation that the correlations of the analysis increment are an overestimation of the analysis error correlations (see Section 4.1).

The first step of the NMC method, which relies on the first analysis increment, thus already emphasizes much more the large-scale features than the ensemble method. Now, the contrast between the two related spectra is similar to what is observed in Fig. 2, which confirms the importance of the

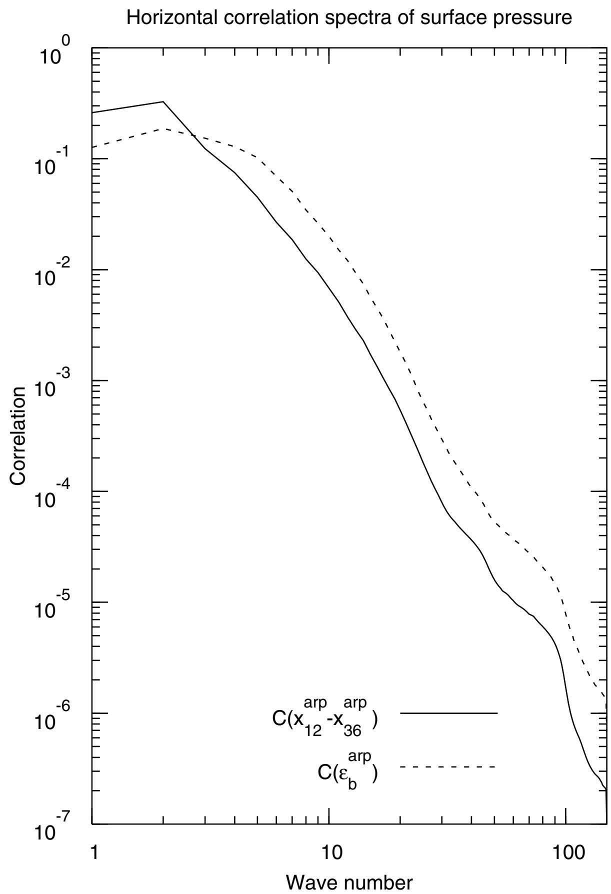

Fig. 2. The Arpège NMC correlation spectrum (full line) compared to the Arpège background ensemble correlation spectrum (dotted line).

analysis representation difference between the two simulation techniques.

To summarize, firstly, it appears that all the three NMC-specific ingredients contribute to the increased emphasis on the large scales in the NMC method. Secondly, the different representations of the analysis step appear to be the strongest contribution to the scale differences between the two simulation techniques.

5.4. The evolution of spectra during an analysis step

The influence of the analysis effect representation can be confirmed by examining what happens during the second analysis step of the NMC method. The left panel of Fig. 4 shows the variance spectrum of the first increment after its 6-h evolution, namely, $M\,\mathrm{d}x^i$, and its modification when adding the second analysis increment $\mathrm{d}x^{i+1}$. It appears that the addition of this second increment implies a general increase of the variances (which is somewhat stronger in the large scales than in the intermediate scales).

There is a strong discrepancy between this variance increase and the modification of the variance spectrum of the background dispersion during the analysis step (in the ensemble method) (right panel of Fig. 4). The analysis contributes to a decrease of the large-scale dispersion, which implies a reduction of the large-scale contributions.

The latter result is consistent with the expectation that the analysis process uses the observations to reduce the amplitude of the large scale part of the background errors.

In other words, the large-scale NMC/ensemble differences are related to the following different evolution processes: the NMC method is strongly based on the analysis increments (and on their accumulation and evolution), while the ensemble method is rather simulating the error reduction during the analysis step.

6. The lagged NMC method

6.1. Description of the method

A variant of the standard NMC method has been used by Široká et al. (2003), in order to derive background error covariances for the Aladin model. This variant has been called the lagged NMC method.

The difference from the standard NMC method concerns the lateral boundary conditions (LBCs) and the initial condition (IC) of the “fresh” 12-h forecast integration. Instead of the usual operational (“fresh”) fields, the LBCs and the IC of the 12-h forecast correspond now to some fields that are derived from the “old” 36-h forecast integration.

More precisely, the LBCs of the 12-h forecast are taken as being identical to those that are used during the last 12-h of integration of the 36-h forecast. Moreover, the IC of the 12-h forecast is now taken as being the coupling field that is involved in the 36-h forecast, at the corresponding time (i.e. for the time $t_1 = t_0 + 24h$, where t_0, t_1 are the respective starting dates of the 36-h and 12-h forecast integrations). A digital filter initialization (DFI) (Lynch and Huang, 1992, and Lynch et al., 1997) is then applied to this coupling field, before the Aladin 12-h forecast integration itself.

Compared to the standard NMC method, the implied forecast differences appeared to have some similar variances in the small scales, but much smaller variances in the large scales (see top panels in Fig. 5).

6.2. The link with the Arpège/Aladin model differences

In this section, it will be shown that the lagged NMC method is closely related to the Arpège/Aladin model differences (although this was not explicit in the original description of the lagged NMC method).

The new IC of the 12-h forecast x_{12}^{ald} is indeed simply the Arpège 24-h forecast x_{24}^{arp}, interpolated onto the Aladin grid, and

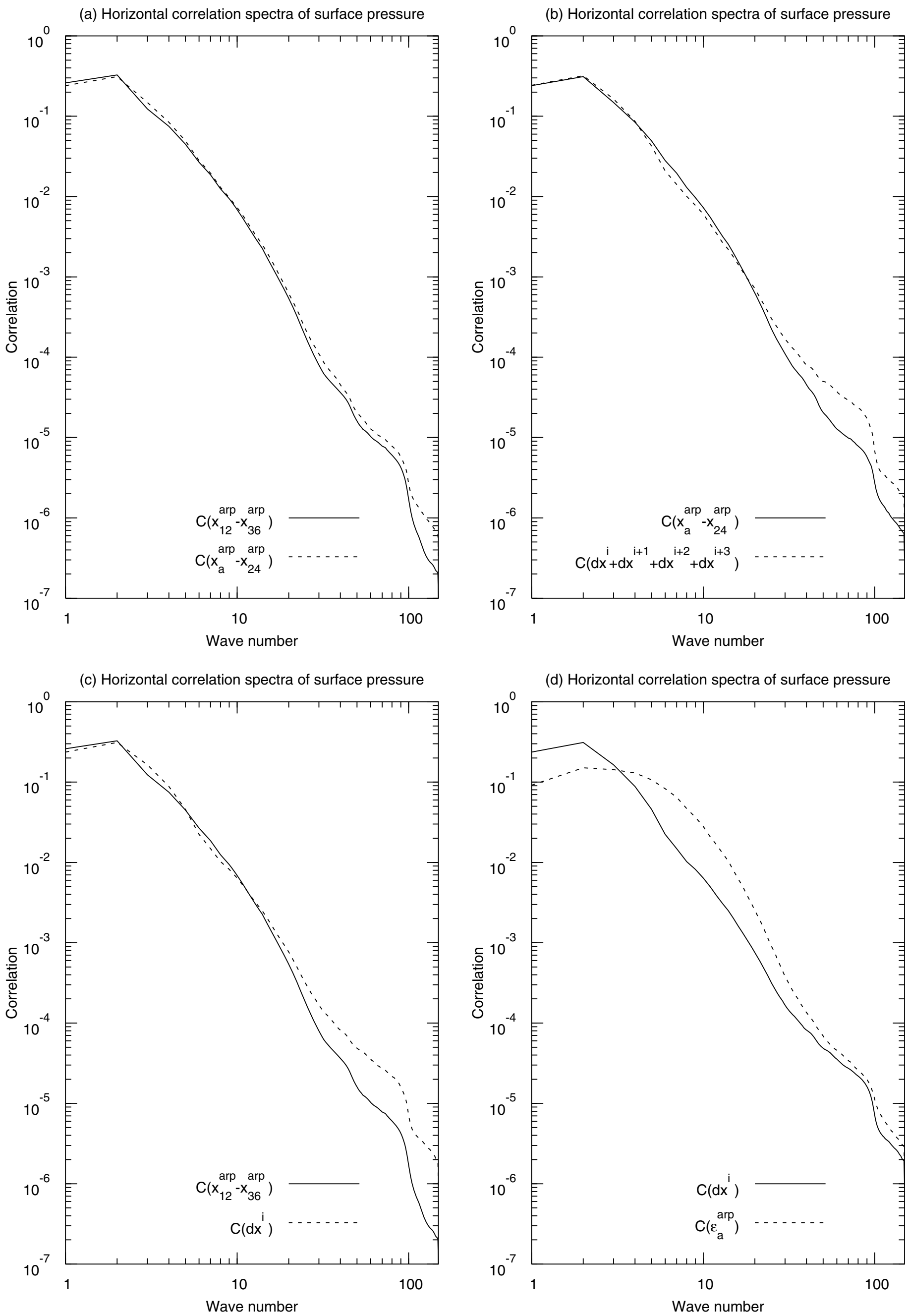

Fig. 3. The error correlation spectra of the following Arpège fields: (a) the 12 h–36 h NMC differences (full line) and the 00 h–24 h NMC differences (dotted line); (b) the 00 h–24 h NMC differences (full line) and the sum of the four (NMC) analysis increments (dotted line); (c) the 12 h–36 h NMC differences (full line) and the first (NMC) analysis increment (dotted line); (d) the first (NMC) analysis increment (full line) and the ensemble analysis differences (dotted line).

initialized by digital filters:

$$x_{12}^{\mathrm{ald}} = \tilde{M}^2 D \tilde{H}\, x_{24}^{\mathrm{arp}},$$

where $\tilde{M}$ is the Aladin 6-h forecast operator, D is the DFI operator and $\tilde{H}$ is the interpolation operator of an Arpège field onto the Aladin grid.

By contrast, the 36-h forecast x_{36}^{ald} can be seen as another 12-h forecast integration, whose IC is an Aladin 24-h forecast x_{24}^{ald}:

$$x_{36}^{\mathrm{ald}} = \tilde{M}^2\, x_{24}^{\mathrm{ald}}.$$

In other words, the final forecast differences correspond to the 12-h forecast evolution of some initial differences, which are the

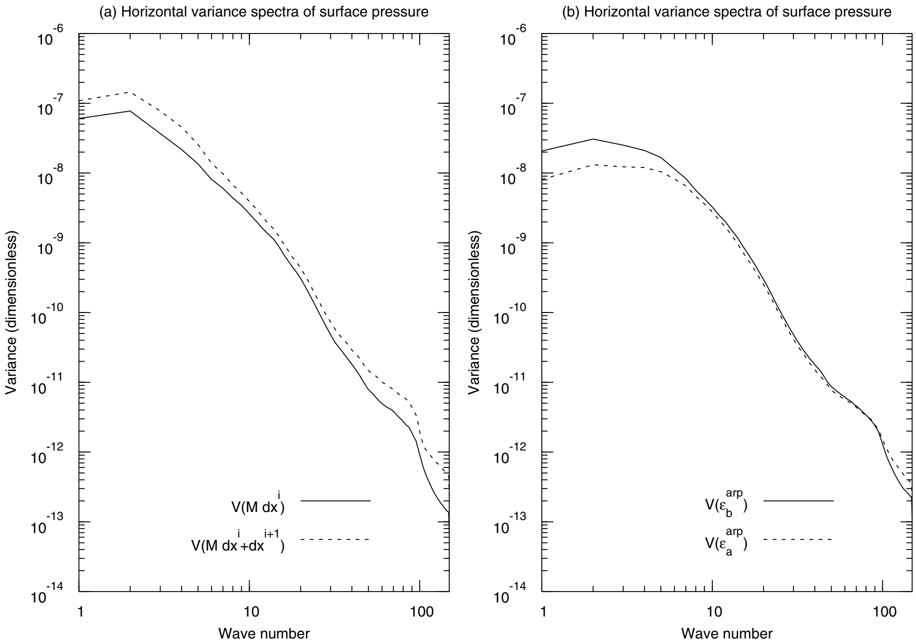

Fig. 4. (a) The evolution of the variance spectra during an analysis step, in the NMC method. This panel shows the variance spectrum of $M\,\mathrm{d}\,x^i$ (full line; this is the first increment, after its six hour evolution), and its modification when adding the second analysis increment $\mathrm{d}\,x^{i+1}$ (dotted line). (b) The evolution of the variance spectra during an analysis step, in the ensemble method. This panel shows the variance spectra of the background differences (full line) and of the analysis differences (dotted line).

differences between an (initialized) Arpège 24-h forecast and an Aladin 24-h forecast:

$$x_{12}^{\mathrm{ald}} - x_{36}^{\mathrm{ald}} = \tilde{M}^2 \left(D\tilde{H}\, x_{24}^{\mathrm{arp}} - x_{24}^{\mathrm{ald}} \right).$$

This means that the initial differences are caused by the differences between the Arpège and Aladin models (which are accumulated over a period of 24 h):

$$D\tilde{H}\, x_{24}^{\mathrm{arp}} - x_{24}^{\mathrm{ald}} = (D\tilde{H} M^4 - \tilde{M}^4 D\tilde{H})\, x_a^{\mathrm{arp}},$$

where M is the Arpège 6-h forecast operator.

Viewing the final forecast differences as being closely related to the Arpège/Aladin model differences may help to interpret some features of the lagged NMC method.

In particular, the correlation spectra of the lagged NMC method are shifted towards the small scales, compared to those of the standard NMC method. This is consistent with the fact that the Arpège/Aladin forecast differences are likely to reflect, to a large extent, the small-scale structures that are represented by Aladin, and not by Arpège.

This appears to be confirmed by the examination of the variance spectra of the differences between the (initialized) Arpège 24-h forecast and the Aladin 24-h forecast (top panels of Fig. 5): the large-scale variances are much smaller than those of the standard NMC method.

The final 12-h forecast integration does not appear to change much the initial variance spectra (except for a small decrease of variance at all scales). This suggests that the essential ingredient of the lagged NMC method is indeed the Arpège/Aladin model differences.

The variance spectra of the Arpège/Aladin 24-h differences were also compared to those of the Arpège/Aladin 6-h differences (bottom panels of Fig. 5). The two additional 18-h integrations appear to increase the large-scale variances, while the small-scale variances remain similar.

6.3. *Comparison between the statistics of the three techniques*

The variance spectra of the following three error simulation techniques can be compared: the ensemble method, the standard NMC method and the lagged NMC method (top panels of Fig. 6). The spectra of the ensemble method appear to be intermediate between those of the two other estimation techniques.

The smaller amplitude of the ensemble large-scale variances, compared to the standard NMC method, is consistent with a more accurate representation (in the ensemble approach) of the influence of the analysis step and of the short forecast ranges (namely, 6 h).

Moreover, the larger amplitude of the ensemble large-scale variances, compared to the lagged NMC method, is consistent with the representation (in the ensemble approach) of the IC and LBC uncertainties. By contrast, the lagged NMC method is in fact based on two assumptions. Firstly, the LBCs are assumed to be perfect. Secondly, the IC uncertainties are assumed to be small: the Arpège and Aladin 24-h forecasts are based on the

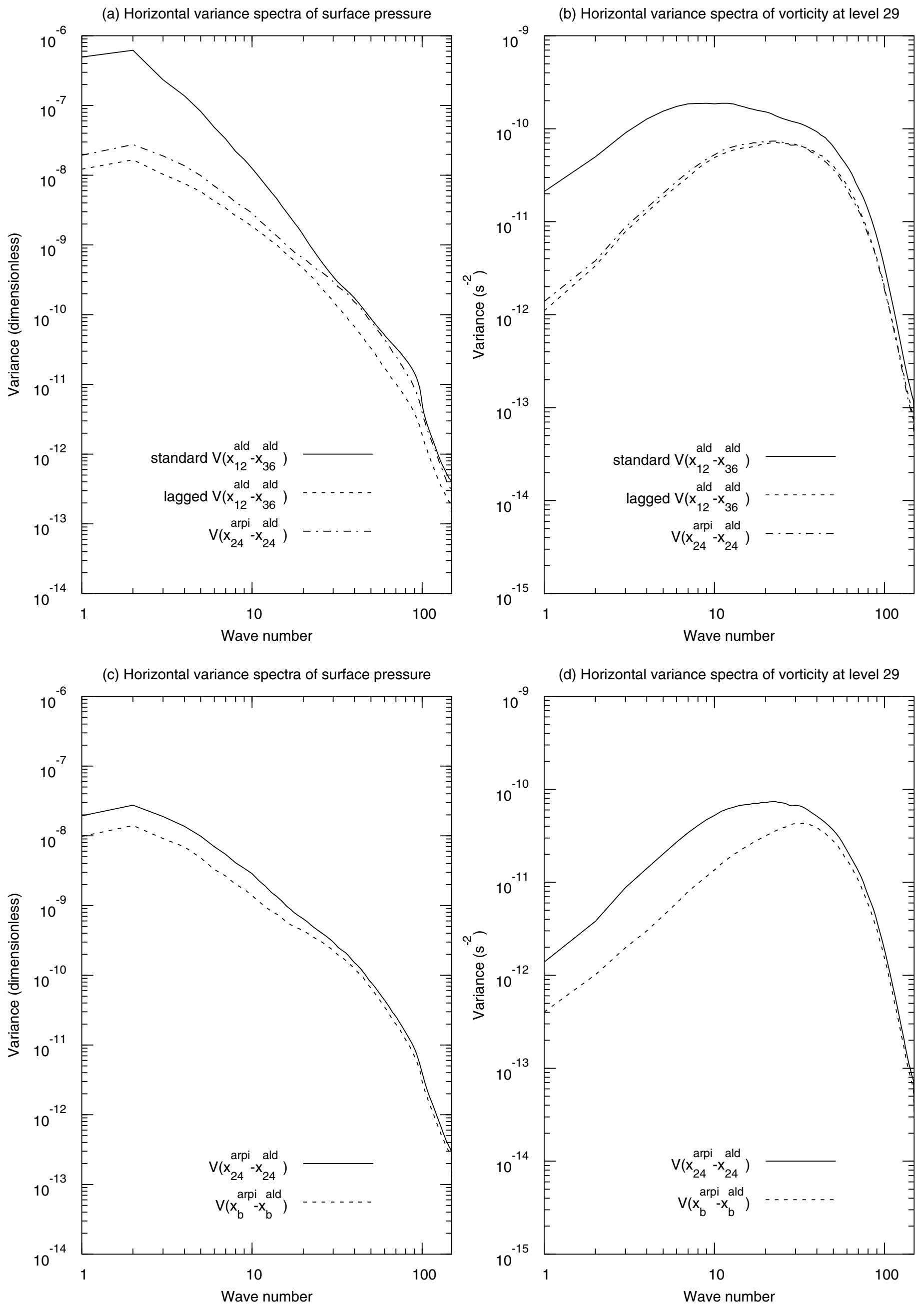

Fig. 5. Top panels: the error variance spectra for the standard (full lines) and lagged (dotted lines) NMC methods, and for the 24 h Arpège/Aladin differences (dash-dotted lines). Bottom panels: the variance spectra of the 24 h (full lines) and 6 h (dotted lines) Arpège/Aladin differences.

same Arpège analysis, and the small Arpège/Aladin 24-h forecast differences may be seen as approximating some rather small IC uncertainties for the additional Aladin 12-h forecast.

The vertical profiles of the length scales (bottom panels of Fig. 6), and of the total standard deviations (Fig. 7), can be examined also. The results are consistent with the variance spectra: the ensemble results appear to be intermediate between those of the two NMC methods. The contrasts are more pronounced for a large-scale variable such as temperature, than for a small-scale variable such as divergence.

7. Conclusions and perspectives

An analysis ensemble approach has been compared, formally and experimentally, with two other error simulation techniques. A formal examination of the model state error evolution has

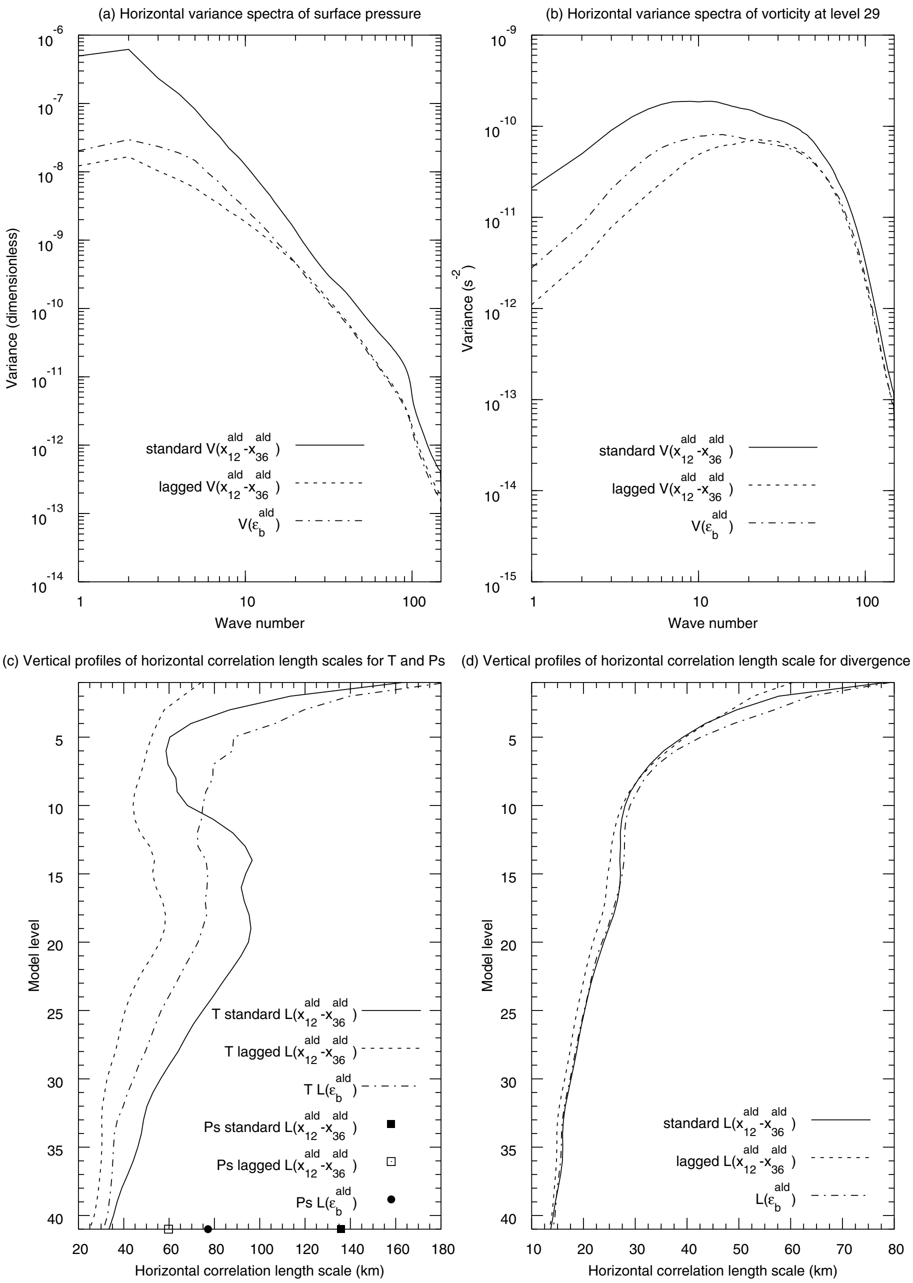

Fig. 6. The error variance spectra (top panels) and the correlation length scales (bottom panels) for the Aladin standard (full lines) and lagged (dotted lines) NMC methods, and for the Aladin background ensemble (dash-dotted lines).

been done first, with respect to the influence of the analysis and forecast steps. It appeared in particular that the analysis equation is the very same equation that transforms the background and observation errors into the analysis errors. This is the case, even if the specified covariance matrices are suboptimal, and even if the observation operator is imperfect.

This allows to notice some strong similarities with the evolution of the ensemble differences, in the ensemble technique. It can be shown that the analysis equation is the equation that transforms the background and observation perturbations into the analysis perturbations. This suggests that the influence of the analysis step is well represented in this ensemble technique.

By contrast, the representation of the analysis step can be shown to be inaccurate in the standard NMC method. Indeed, this estimation technique relies essentially on the accumulation and the evolution of some analysis increments. Two results confirm that this process of analysis increment accumulation is not a good approximation of the analysis process.

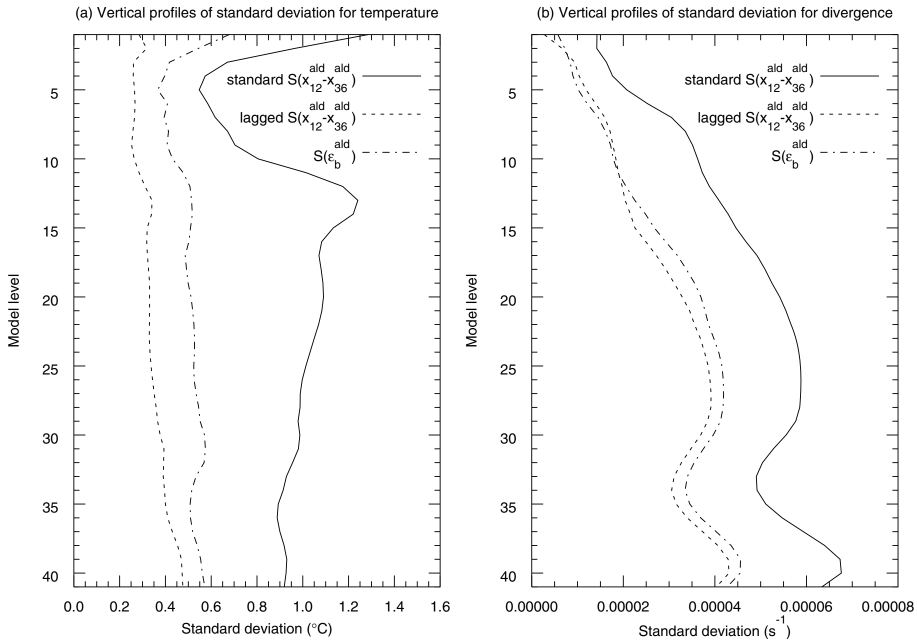

Fig 7. The vertical profiles of the standard deviations for the Aladin standard (full lines) and lagged (dotted lines) NMC methods, and for the Aladin background ensemble (dash-dotted lines).

Firstly, the filtering properties of the gain matrix **K** imply that the analysis increment is expected to be of a larger scale than the analysis error. This is supported experimentally by the comparison with the analysis dispersion spectrum. Moreover, this difference appears to be one of the main contributions to the larger-scale spectra in the NMC method (compared to the ensemble method).

Secondly, another related experimental result is that the analysis increment accumulation implies an increase of variance for all scales, while the analysis process contributes to a decrease of the large-scale dispersion (as expected, in particular, over a data-rich region such as the Aladin-France domain).

The representation of the initial errors and of the analysis effect is even more poor in the so-called lagged NMC method. This variant appeared in fact to be closely related to the Arpège/Aladin model differences. This suggests that some ingredients of the lagged NMC method, such as the latter model differences, may rather be used in order to estimate the contributions of some of the involved model errors. The close link between the lagged NMC method, and the Arpège/Aladin model differences, also explains why the implied forecast difference spectra are shifted towards smaller scales.

The variance spectra of the Aladin background errors provided by the ensemble method were compared to those of the other two techniques. The ensemble spectra were found to be intermediate. Compared to the lagged NMC method, the amplitudes of the large-scale variances are increased: this is consistent with the representation, in the ensemble method, of the influence of the initial and lateral boundary conditions uncertainties. These large-scale ensemble variances are however smaller than those of the standard NMC method: this is consistent with the more accurate representation (in the ensemble approach) of the analysis step and of the short forecast ranges.

Due to this accurate representation of the analysis and forecast effects, the ensemble method will be used to specify the corresponding error statistics of the Aladin 3D-Var. The latter may include a term which will control the distance to the Arpège analysis (Bouttier, 2002).

Moreover, these Aladin 3D-Var analyses will allow to compare the Aladin background and the Arpège analysis with the available observations. This will also give the possibility to calculate the corresponding departures of the two model states from observations. The statistics of these departures, and more generally, the use of a posteriori diagnostics (e.g. Desroziers and Ivanov, 2001; Sadiki and Fischer, 2005) may also provide some complementary estimates of the error statistics.

The introduction of model perturbations may help to increase further the realism of the ensemble simulation. In a forthcoming publication, a first step towards this will be described, which relies on a detailed examination of the Arpège/Aladin model differences.

Finally, the present study deals with some time- and space-averaged error covariances. Time- and space-dependent features may be explored in the future, for example, by integrating a larger number of ensemble members, and/or for instance by relating the error structures to the background field structures. Moreover, it may be particularly attractive to use wavelets in this context, both on the globe (Fisher, 2003) for Arpège and in a limited area (Deckmyn and Berre, 2005) for Aladin: this would allow to diagnose and to specify the local error structures.

8. Acknowledgments

The authors would like to thank François Bouttier, François Bouyssel, Claude Fischer, Jean Maziejewski and Alex Deckmyn for carefully reading the early versions of the manuscript. We would like also to thank Robert Mureau for his constructive comments, which have enabled to strengthen the structure of the paper. Simona Ecaterina Ştefănescu and Margarida Belo Pereira are grateful to Météo France for supporting their stays in CNRM/GMAP.

9. Appendix: design of the observation and model perturbations in the analysis ensemble approach

The evolution of the model state errors and of the ensemble differences have been examined in Sections 2 and 3. The ensemble approach may thus be summarized as follows, e.g. in the perfect model case.

The forecast model is applied to, for example, two perturbed analyses, which provides two backgrounds for the next analysis time. The analysis scheme is then applied to these two perturbed backgrounds, and to two sets of perturbed observations. This provides two new perturbed analyses, and so on. This process ensures that the ensemble perturbations evolve in a similar way as the model state errors.

Beyond this representation of the 6-h forecast and analysis effects, some additional choices are introduced, in order to achieve a realistic error covariance estimation.

If one drops the time index notation, the equation of the analysis error can be expressed as follows:

$$e_a = (\mathbf{I} - \mathbf{K}H)e_b + \mathbf{K}e_o,$$

where $\mathbf{I}$ is the identity matrix. This implies the following expression for the associated exact error covariance matrices, namely, the analysis error covariance matrix $\mathbf{A}_* = \overline{e_a(e_a)^T}$, the background error covariance matrix $\mathbf{B}_* = \overline{e_b(e_b)^T}$ and the observation error covariance matrix $\mathbf{R}_* = \overline{e_o(e_o)^T}$ (if $\overline{e_b(e_o)^T} = 0$, where the overbar corresponds to an ensemble average):

$$\mathbf{A}_* = (\mathbf{I} - \mathbf{K}H)\mathbf{B}_*(\mathbf{I} - \mathbf{K}H)^T + \mathbf{K}\mathbf{R}_*\mathbf{K}^T.$$

Similarly, the equation of the analysis ensemble difference (between two members) is the following:

$$\varepsilon_a = (\mathbf{I} - \mathbf{K}H)\varepsilon_b + \mathbf{K}\varepsilon_o,$$

which implies the following expression for the associated ensemble difference covariance matrices, $\mathbf{A}_\varepsilon = \overline{\varepsilon_a(\varepsilon_a)^T}$, $\mathbf{B}_\varepsilon = \overline{\varepsilon_b(\varepsilon_b)^T}$ and $\mathbf{R}_\varepsilon = \overline{\varepsilon_o(\varepsilon_o)^T}$ (if $\overline{\varepsilon_b(\varepsilon_o)^T} = 0$):

$$\mathbf{A}_\varepsilon = (\mathbf{I} - \mathbf{K}H)\mathbf{B}_\varepsilon(\mathbf{I} - \mathbf{K}H)^T + \mathbf{K}\mathbf{R}_\varepsilon\mathbf{K}^T. \tag{7}$$

In practice, the two sets of observation perturbations are obtained as random realizations of the Gaussian probability distribution function (pdf) whose mean is zero, and whose covariance matrix corresponds to the specified observation error covariance matrix $\mathbf{R}$:

$$\delta_{o,k}, \delta_{o,l} \sim \mathcal{N}(0, \mathbf{R}),$$

that is, $\overline{\delta_{o,k}(\delta_{o,k})^T} = \overline{\delta_{o,l}(\delta_{o,l})^T} = \mathbf{R}$.

These two random realizations are uncorrelated, which implies that the covariance matrix of the observation difference $\varepsilon_o = \delta_{o,k} - \delta_{o,l}$ is equal to twice the specified covariance matrix $\mathbf{R}$:

$$\begin{aligned}\mathbf{R}_\varepsilon &= \overline{\varepsilon_o(\varepsilon_o)^T} \\ &= \overline{\delta_{o,k}(\delta_{o,k})^T} + \overline{\delta_{o,l}(\delta_{o,l})^T} - \overline{\delta_{o,k}(\delta_{o,l})^T} - \overline{\delta_{o,l}(\delta_{o,k})^T} \\ &= 2\,\mathbf{R}.\end{aligned}$$

If the specified observation error covariance matrix $\mathbf{R}$ is a good approximation of the exact observation error covariance matrix $\mathbf{R}_*$, namely, $\mathbf{R} \approx \mathbf{R}_*$, then one obtains:

$$\mathbf{R}_\varepsilon = 2\,\mathbf{R}_*. \tag{8}$$

Similarly, the background difference ε_b can be seen as the difference between two background perturbations (that are relative to an unperturbed background x_b): $\delta_{b,k} = x_{b,k} - x_b$, $\delta_{b,l} = x_{b,l} - x_b$, and $\varepsilon_b = \delta_{b,k} - \delta_{b,l}$.

If these two background perturbations are uncorrelated, and if their spatial covariances are those of the exact background error covariance matrix $\mathbf{B}_*$, then the covariance matrix of ε_b will be twice the exact error covariance matrix:

$$\mathbf{B}_\varepsilon = \overline{\varepsilon_b(\varepsilon_b)^T} = 2\,\mathbf{B}_*. \tag{9}$$

By replacing these expressions of $\mathbf{R}_\varepsilon$ and $\mathbf{B}_\varepsilon$ in the eq. (7), one obtains:

$$\mathbf{A}_\varepsilon = 2\,\mathbf{A}_*. \tag{10}$$

In other words, the covariances of the analysis ensemble differences are expected to be equal to twice the covariances of the analysis errors.

As shown above for the observations, the factor 2 results from the construction of perturbations that are mutually uncorrelated (between different members), and whose (spatial) covariances are made to approximate the error covariances.

A similar principle applies to the possible model perturbations ε_m: the specific model perturbation $\delta_{m,k}$ of a given member k should ideally be mutually uncorrelated with the model perturbation of any other member, and for example, its variance should approximate the variance of the model error e_m.

References

Bouttier, F. 1994. *Sur la prévision de la qualité des prévisions météorologiques*. PhD Dissertation. Université Paul Sabatier, Toulouse, 240 pp. [Available from Université Paul Sabatier, Toulouse Cedex, France].

Bouttier, F. 2002. Strategies for kilometric-scale LAM data assimilation. In: *Report of HIRLAM Workshop on Variational Data Assimilation and Remote Sensing*, Helsinki, 21–23 January 2002, Finnish Meteorological Institute, 9–17. [Available from SMHI, S-60176 Norrköping, Sweden].

Bubnová, R., Horányi, A. and Malardel, S. 1993. International project ARPEGE/ALADIN. *EWGLAM Newsl.* **22**, 117–130.

Daley, R. 1991. *Atmospheric Data Analysis*. Cambridge University Press, Cambridge, 460 pp.

Deckmyn, A. and Berre, L. 2005. A wavelet approach to representing background error covariances in a limited area model. *Mon. Weather Rev.* **133**, 1279–1294.

Desroziers, G. and Ivanov, S. 2001. Diagnosis and adaptive tuning of information error parameters in a variational assimilation. *Q. J. R. Meteorol. Soc.* **127**, 1433–1452.

Fisher, M. 2003. Background error covariance modelling. In: *Proceedings of the ECMWF Seminar on Recent Developments in Data Assimilation for Atmosphere and Ocean*, ECMWF, 8–12 September 2003, 45–63. [Available from ECMWF, Reading, RG2 9AX, UK]

Houtekamer, P. L., Lefaivre, L., Derome, J., Ritchie, H. and Mitchell, H. L. 1996. A system simulation approach to ensemble prediction. *Mon. Weather Rev.* **124**, 1225–1242.

Lynch, P. and Huang, X.-Y. 1992. Initialization of the HIRLAM model using a digital filter. *Mon. Weather Rev.* **120**, 1019–1034.

Lynch, P., Giard, D. and Ivanovici, V. 1997. Improving the efficiency of a digital filtering scheme for diabatic initialization. *Mon. Weather Rev.* **125**, 1976–1982.

Parrish, D. F. and Derber, J. C. 1992. The National Meteorological Center's spectral statistical interpolation analysis system. *Mon. Weather Rev.* **120**, 1747–1763.

Radnóti, G., Ajjaji, R., Bubnová, R., Caian, M., Cordoneanu, E. and Coauthors, 1995. The spectral limited area model ARPEGE/ALADIN. *PWPR Rep. Ser.* **7**, *WMO-TD* **699**, 111–117.

Sadiki, W. and Fischer, C. 2005. A posteriori validation applied to the 3D-Var Arpège and Aladin data assimilation systems. *Tellus* **57A**, 21–34.

Široká, M., Fischer, C., Cassé, V., Brožkova, R. and Geleyn, J.-F. 2003. The definition of mesoscale selective forecast error covariances for a limited area variational analysis. *Meteorol. Atmos. Phys.* **82**, 227–244.

Veersé, F. and Thépaut, J.-N. 1998. Multiple-truncation incremental approach for four-dimensional variational data assimilation. *Q. J. R. Meteorol. Soc.* **124**, 1889–1908.

Žagar, N., Andersson, E. and Fisher, M. 2004. Balanced tropical data assimilation based on a study of equatorial waves in ECMWF short-range forecast errors. *ECMWF Tech. Memo.* **437**, 30 pp.